

Kinetic Potential and Barrier Crossing: A Model for Warm Cloud Drizzle Formation

Robert McGraw and Yangang Liu

Environmental Sciences Department, Atmospheric Sciences Division, Brookhaven National Laboratory, Upton, New York 11973
(Received 21 June 2002; published 9 January 2003)

The kinetic potential of nucleation theory is used to describe droplet growth processes in a cloud. Drizzle formation is identified as a statistical barrier-crossing phenomenon that transforms cloud droplets to drizzle size with a rate dependent on turbulent diffusion, droplet collection, and size distribution. Steady-state and transient drizzle rates are calculated for typical cloud conditions. We find drizzle more likely under transient conditions. The model quantifies an important indirect effect of aerosols on climate-drizzle suppression in clouds of higher droplet concentration.

DOI: 10.1103/PhysRevLett.90.018501

PACS numbers: 92.60.Nv, 47.55.Dz, 82.60.Nh

Clouds and precipitation play crucial roles in regulating Earth's energy balance and water cycle [1]. Although it has been well established that three basic physical processes (nucleation, condensation, and collection) are involved in the formation of warm rain where the ice phase plays no role, many issues regarding the initiation of warm rain remain unsolved [2–5]. One of the fundamental problems that has long frustrated the cloud physics community is an explanation for the production of droplets with radii around 20 μm . On one hand, classical condensation theory cannot adequately explain the formation of these droplets because of their slow condensation growth rate. On the other hand, for water droplets falling in still air, growth by collection is very slow until some droplets have reached radii in excess of 20 μm [6]. For example, Jonas [3] calculated droplet growth by condensation and collection in still air, and found that the growth of a droplet from 10 μm radius to 20 μm by condensation at a typical supersaturation of 0.2% takes about 20 min while growth by collection from 20 μm to drizzle drops ($\sim 100 \mu\text{m}$ radius) in a cloud with a liquid water content of 1 g m^{-3} would take 1 h. The combined growth time is much greater than the lifetime of typical precipitation cumulus clouds ($\sim 30 \text{ min}$). Much progress has been made over the last few decades, especially in understanding the role of cloud turbulence, which is believed to enhance both condensation growth and the collection process by small droplets [2–5]. Nevertheless, the details of these turbulent effects remain illusive and highly controversial. In this Letter we attack this problem by extending the theory of statistical crossing of a kinetic barrier in nucleation to the processes of condensation and collection. The new theory admits a critical droplet size, here approximately 20–30 μm in radius, having balanced condensation, collection, and evaporation rates. We show that significant drizzle rates can occur even though cloud lifetimes may be too short to reach steady state.

Consider the nucleation of a water droplet containing g molecules, whereby single molecules are exchanged with a surrounding vapor, and each step can be represented by

the equilibrium:

$$A_g + A_1 = A_{g+1}, \quad (1)$$

where A_1 represents the water vapor monomer and A_g a drop of size g . Under conditions of stable or (constrained) metastable equilibrium, detailed balance gives

$$\beta_g n_g = \gamma_{g+1} n_{g+1}, \quad (2)$$

where β_g (s^{-1}) is the rate of monomer condensation on the drop, γ_g the corresponding evaporation rate, and n_g (cm^{-3}) is the constrained equilibrium concentration of drops of size g . According to Eq. (2), n_g can be written in the product form:

$$\begin{aligned} n_g &= n_1 \frac{n_2}{n_1} \frac{n_3}{n_2} \dots \frac{n_{g-1}}{n_{g-2}} \frac{n_g}{n_{g-1}} \\ &= n_1 \frac{\beta_1}{\gamma_2} \frac{\beta_2}{\gamma_3} \dots \frac{\beta_{g-2}}{\gamma_{g-1}} \frac{\beta_{g-1}}{\gamma_g} = n_1 \prod_{i=1}^{g-1} \frac{\beta_i}{\gamma_{i+1}}. \end{aligned} \quad (3)$$

Alternatively, in Boltzmann form,

$$n_g = n_1 \exp[-W(g)/kT], \quad (4)$$

where $W(g)/kT$ is the reduced thermodynamic potential for droplet formation from the vapor. Combination of Eqs. (3) and (4) gives

$$\frac{W(g)}{kT} = -\ln\left(\prod_{i=1}^{g-1} \frac{\beta_i}{\gamma_{i+1}}\right) \equiv \Phi(g), \quad (5)$$

where $\Phi(g)$ is the kinetic potential [7].

The kinetic and reduced thermodynamic potentials are equivalent in nucleation theory. However, the kinetic potential is more general in that it is defined solely in terms of rate constants, even in the absence of a well-defined equilibrium condition. Here the kinetic potential is applied to study the initiation of warm rain. The growth of cloud droplets is represented as a sum of contributions from condensation and collection processes:

$$\beta_g = \beta_g^{\text{cond}} + \beta_g^{\text{coll}}. \quad (6)$$

Collection refers to the enhanced growth of those rare droplets large enough to have a gravitational fall speed that allows aggregation with smaller, typical cloud size droplets in the 10 μm radius range.

We first consider the rate for condensation growth β_g^{cond} . Describing evaporation and growth as random events results in Brownian-like fluctuations along the g coordinate and a distribution of droplet sizes. For cloud droplets these fluctuations will be similar to fluctuations in molecular cluster size during nucleation [8], but on the much larger scale of turbulent fluctuations in growth rate. The diffusion coefficient in number space is $D = \alpha l^2/2$ and has units of s^{-1} where α is the total number of displacements per unit time (with both forward and reverse jumps counted) and l is the number of molecules per jump [9]. For single-molecule jumps $l = 1$ and $D(g) = \beta_g^{\text{cond}}$ for equal forward and reverse rates [8]. The mean square displacement after time t is $\sigma_g^2 = 2Dt$. Consider a 1% change in drop radius from 10 to 10.1 μm resulting in an increase in the number of molecules present in the drop by $\Delta g = 4.2 \times 10^{12}$ occurring diffusively on the time scale $t_{1\%} = (\Delta g)^2/2\beta_g^{\text{cond}}$. We determine β_g^{cond} through the assignment of a reasonable range of values to $t_{1\%}$. For example, for $t_{1\%} = 1$ s we obtain the *effective* diffusion coefficient, $D = \beta_g^{\text{cond}} = 9 \times 10^{24} \text{ s}^{-1}$. For comparison, diffusion-controlled growth of a cloud droplet under a supersaturation of 0.2%, a typical value for the fluctuating supersaturation in cloud, gives a $t_{1\%}$ of about 1 s. We will parametrize the effects of turbulence on cloud droplet growth using values of $t_{1\%}$ in the range 0.1–10 s, and treat β_g^{cond} as size independent. Longer times would not allow for significant fluctuations in drop size over the lifetime of a cloud and shorter times would imply growth rates faster than are likely to occur for the typical range of supersaturation found in clouds.

Next, we need to represent the complicated interactions between cloud droplets due, for example, to the competition for available water vapor. For this, we introduce an effective evaporation rate γ_g^{eff} determined from β_g^{cond} so as to yield a reasonable cloud droplet distribution through detailed balance. Examination of typical cloud droplet distributions [10,11] shows that these are well approximated by a maximum entropy distribution subject to the constraint that total liquid water per unit volume is conserved. This gives the exponential form [10]:

$$n_g = \frac{N_D}{a} \exp(-g/a), \quad (7)$$

where N_D is the number of droplets per cm^3 and $1/a$ is a parameter controlling the falloff of the distribution. For an average particle radius of 10 μm , $a = 1.67 \times 10^{14}$. The drop volume fraction is $L = N_D a \nu_1$. For small droplets ($g \ll a$) the concentration for each size g approaches N_D/a , an important boundary condition for calculating the drizzle rate. Substitution of Eq. (7) into the detailed balance condition [Eq. (2)] gives

$$\frac{n_{g+1}}{n_g} = \frac{\beta_g^{\text{cond}}}{\gamma_{g+1}^{\text{eff}}} \approx \frac{\beta_g^{\text{cond}}}{\gamma_g^{\text{eff}}} = \exp(-1/a), \quad (8)$$

where the last equality defines the effective evaporation rate.

Finally, we turn to the collection process. The rate of volumetric gain of a specified drop of volume x falling through a population of smaller droplets, having volume distribution function $f(y)$, is given by

$$\frac{dx}{dt} = \int_0^\infty K(x, y) y f(y) dy. \quad (9)$$

The collection kernel depends generally on the collection efficiency E and the terminal velocity V and is given by [6]

$$K(x, y) = E(x, y) \pi \left[\left(\frac{3x}{4\pi} \right)^{1/3} + \left(\frac{3y}{4\pi} \right)^{1/3} \right]^2 [V(x) - V(y)]. \quad (10)$$

Collection is represented, according to Eq. (9), as a single-particle growth process that takes place in a medium of the smaller cloud droplets specified by $f(y)$. For collector drops of radius less than 50 μm the kernel is well approximated [12] by $K(x, y) = 1.1 \times 10^{10} x^2$, where K has units of $\text{cm}^3 \text{ s}^{-1}$. Substitution in Eq. (9) gives

$$\frac{dx}{dt} = 1.1 \times 10^{10} x^2 L, \quad (11)$$

where $L = \int_0^\infty y f(y) dy$ is the cloud liquid water volume fraction. Converting to an effective collection rate gives

$$\beta_g^{\text{coll}} \equiv \frac{dg}{dt} = \frac{1}{\nu_1} \frac{dx}{dt} = 3.3 \times 10^{-13} g^2 L, \quad (12)$$

where $\nu_1 = 3.0 \times 10^{-23} \text{ cm}^3$ is the molecular volume of liquid water. It is safe to assume that the collection process does not affect the evaporation rate because no significant breakup occurs for drops of this size. Equations (8) and (12) and the assignment of $t_{1\%}$ fully determine the rate constants and kinetic potential [Eqs. (5) and (6)] for the model.

Figure 1 shows the kinetic potential as a function of drop radius. Results are for a cloud drop volume fraction of 5×10^{-7} (equal to 0.5 g m^{-3}) for a liquid water density $\rho = 1 \text{ g cm}^{-3}$, and droplet number densities of 100 and 300 cm^{-3} corresponding to average cloud droplet radii of 10.6 and 7.4 μm , respectively. The inset shows a simulation of growth fluctuations for a subcritical 10 μm drop under these conditions obtained using a stochastic model [9]. Solid and dashed curves are the potentials with and without collection, respectively. The potential maximum defines a critical droplet radius, r^* , for which the forward and reverse growth rates are in balance, $\beta_g^{\text{cond}} + \beta_g^{\text{coll}} = \gamma_g^{\text{eff}}$. Figure 1 shows the dramatic effect of a decrease in droplet concentration on lowering the kinetic barrier and shifting r^* to a smaller size, making rain more easy to

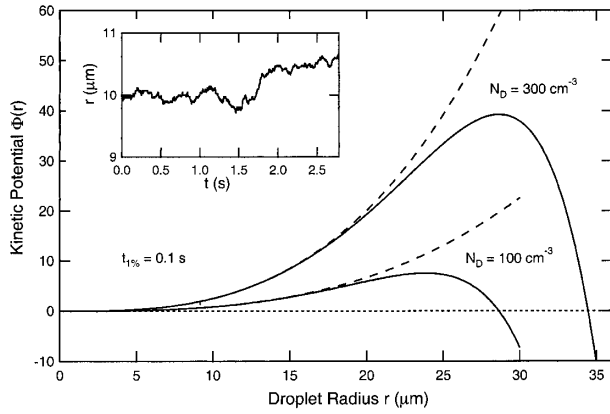


FIG. 1. Kinetic potential with (full curves) and without (dashed curves) collection for $t_{1\%} = 0.1$ s. Results are for a cloud liquid water content of 0.5 g m^{-3} and two different droplet number concentrations. The inset shows fluctuations in single drop size in the precollection regime.

occur in maritime, unpolluted clouds. Squires [13] proposed that continental clouds are colloiddally more stable than their maritime counterparts because of a higher aerosol (hence droplet) concentration and a smaller average droplet size. This hypothesis also serves as the microphysical basis for the second indirect effect of anthropogenic aerosols on climate change [14]. The kinetic potential places this hypothesis on solid physical ground.

The steady-state barrier-crossing rate ($\text{cm}^{-3} \text{ s}^{-1}$) can be obtained, as in classical nucleation theory, using the Becker-Döring kinetics model [15]:

$$J_{ss} = \left(\sum_g \frac{1}{\beta_g n_g} \right)^{-1} = n_1 \sum_g \frac{1}{\beta_g \exp[-\Phi(g)]} \\ = \frac{N_D}{a} \sum_g \frac{1}{\beta_g \exp[-\Phi(g)]}, \quad (13)$$

where the last equality applies to the droplet distribution of Eq. (11). Replacing the sum by an integral and evaluating J gives the results shown in Fig. 2. As in nucleation [15], the steady rate of Eq. (13) is independent of the upper limit of summation so long as this is chosen to be sufficiently larger than the critical size that any return flux can be neglected.

To obtain the induction time for drizzle formation we compute the transient barrier-crossing rate $J(t)$ defined as the flux ($\text{cm}^{-3} \text{ s}^{-1}$) across an arbitrary, but fixed postcritical drop radius, r_G . At $t = 0$, the cloud droplet distribution is assumed to be specified by Eq. (11), which is the equilibrium distribution in the absence of collection. Collection is turned on at this time and the subsequent transient behavior, as $J(t)$ increases from zero to its steady-state value, is shown in Fig. 3 for $r_G = 40 \text{ μm}$. These results were obtained for the present model using a matrix approach previously developed to study transient

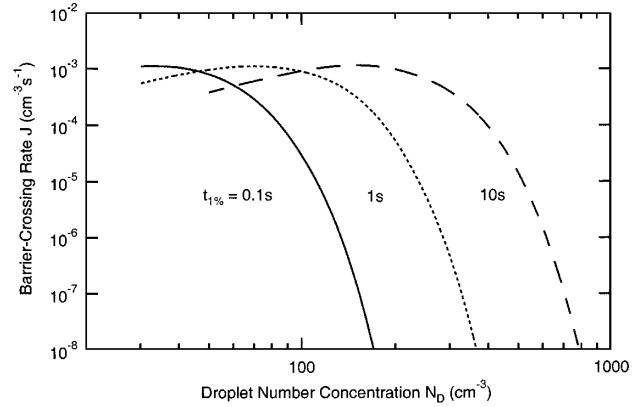


FIG. 2. Steady-state barrier transmission current ($\text{cm}^{-3} \text{ s}^{-1}$). Results are for a cloud liquid water content of 0.5 g m^{-3} and three different values of the turbulent condensation growth rate.

nucleation [8,16]. This requires solving for the eigenvalues and eigenvectors of a Hermitian matrix, \mathbf{H} , of order equal to the number of distinct clusters included in the calculation. In the present application this requires a greatly reduced subsampled array of droplet sizes with appropriately renormalized interactions. Subsampling by a factor of h gives for diffusive transport along the array $\beta_d^{\text{cond}} = \beta_g^{\text{cond}}/h^2$ where now $g_i = h d_i$. With this renormalization of the condensation growth rate, the diffusion constant $D^{(h)}$ is invariant to representation ($D^{(h)} = \beta_d^{\text{cond}} l^2 = h^2 \beta_d^{\text{cond}} = h^2 \beta_g^{\text{cond}}/h^2 = \beta_g^{\text{cond}} = D$) as required. Other observables including the barrier-crossing rate are also invariant under this renormalization of the condensation rate. Collection is a ballistic growth process that takes place on the subsampled lattice at a linearly reduced rate $\beta_d^{\text{coll}} = \beta_g^{\text{coll}}/h$. These renormalized parameters together with the subsampled droplet population $n_d^{(h)} = h n_g$ comprise the elements of \mathbf{H} , from which the time-dependent barrier-crossing rate is obtained. We choose h such the number of sampled droplets (equal to the order of \mathbf{H}) is about 100. Results from the transient calculations are presented in Fig. 3 at two different cloud liquid water loadings. The approach to steady state is faster (shorter induction time) at the higher loading in part because of the larger initial droplet size (see caption). These and other calculations suggest that while drizzle formation is not likely to reach a steady-state rate on the (~ 1 h) lifetime of a typical cloud, a significant fraction of the steady-state formation rate can occur.

For practical applications it is useful to express results in terms of the total rate of drizzle formation in a vertical column of cloud. A convenient measure is cloud liquid water path (LWP). For a uniform cloud the column rate is $R(\text{cm}^{-2} \text{ s}^{-1}) = 10^{-4} J \times \text{LWP}/\rho L$ for LWP in g m^{-2} . Cloud LWP's inferred from satellite measurements vary greatly, tending to cluster in the $50\text{--}300 \text{ g m}^{-2}$ range [17,18]. Drizzle rate from stratocumulus clouds could be

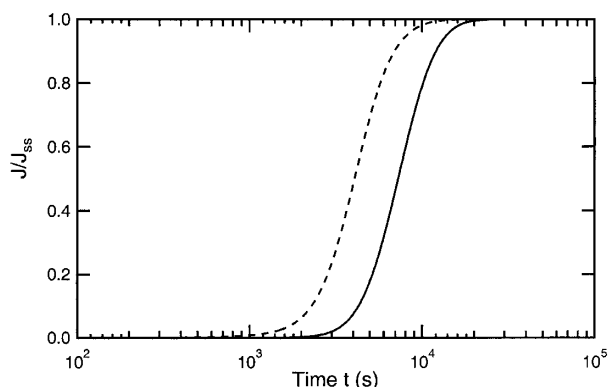


FIG. 3. Transient barrier transmission rate divided by the steady-state rate versus log time in sec. The initial cloud droplet distribution follows Eq. (11), which is the Boltzmann distribution in the absence of collection. Collection is turned on at $t = 0$ and the subsequent transient behavior during the approach to steady state is shown in the figure. Results are for $t_{1\%} = 0.1$ s, $N_D = 100$, and cloud liquid water content (LWC) of 0.5 g m^{-3} (solid curve) and 1.0 g m^{-3} (dashed curve). Under these conditions $J_{ss} = 3 \times 10^{-5} \text{ cm}^{-3} \text{ s}^{-1}$ for $\text{LWC} = 0.5 \text{ g m}^{-3}$ and 4×10^{-3} for $\text{LWC} = 1.0 \text{ g m}^{-3}$.

as small as $\approx 0.01 \text{ mm h}^{-1}$ and as large as $\approx 1 \text{ mm h}^{-1}$ [19,20]. Thus observable rates of drizzle formation, assuming a radius of $100 \mu\text{m}$ for the collected droplets, require $J \geq 10^{-6}$ to $10^{-5} \text{ cm}^{-3} \text{ s}^{-1}$. From Figs. 2 and 3, we see that such rates will occur most frequently for clouds having fewer drops and after an appreciable lag time, depending on the liquid water content of the cloud.

This Letter demonstrates application of the kinetic potential beyond the nucleation field where it is usually applied. Here the kinetic potential has been used in the formulation of a new model for warm rain initiation—a nonequilibrium model for which only the forward and reverse rates of a sequence of elementary reaction steps are known. The new model is consistent with results from the traditional models and with observations of significant indirect effect that aerosols have on climate; by increasing cloud droplet number density, aerosols suppress rain [21]. It also reveals that continental (polluted) clouds are more colloiddally stable because they have a higher kinetic barrier and larger critical droplet sizes compared to their maritime counterparts. Future developments of the model should attempt to include the effects of turbulence on cloud droplet size distribution and collection kernel [22]. In addition to this particular prob-

lem, the methods described here may be useful elsewhere that phenomena viewed as related to nucleation arise.

This research was supported by NASA through interagency agreement number W-18,429 as part of its interdisciplinary research program on tropospheric aerosols and by the Environmental Sciences Division of the U.S. Department of Energy, as part of the Atmospheric Chemistry Program under Contract No. DE-AC02-76CH00016, and the Atmospheric Radiation Measurements Program under Contract No. DE-AC03-98CH10886. The authors thank Dr. Stephen E. Schwartz of BNL for helpful discussions.

-
- [1] M. B. Baker, *Science* **276**, 1072–1078 (1997).
 - [2] K. V. Beard and H. T. Ochs, *J. Appl. Meteor.* **32**, 608–625 (1993).
 - [3] P. R. Jonas, *Atmos. Res.* **40**, 283–306 (1996).
 - [4] J. W. Telford, *Atmos. Res.* **40**, 261–282 (1996).
 - [5] M. B. Pinsky and A. P. Khain, *J. Aerosol Sci.* **28**, 1177–1214 (1997).
 - [6] H. R. Pruppacher and J. D. Klett, *Microphysics of Clouds and Precipitation* (Kluwer Academic, Boston, 1997).
 - [7] D. T. Wu, *Solid State Phys.* **50**, 37–187 (1997).
 - [8] R. McGraw, *J. Phys. Chem. B* **105**, 11 838–11 848 (2001).
 - [9] S. Chandrasekhar, in *Selected Papers on Noise and Stochastic Processes*, edited by N. Wax (Dover, New York, 1954).
 - [10] Y. Liu, L. You, W. Yang, and F. Liu, *Atmos. Res.* **35**, 201–216 (1995).
 - [11] A. Costa, C. Oliveira, J. Oliveira, and A. Sampaio, *Atmos. Res.* **54**, 167 (2000).
 - [12] A. B. Long, *J. Atmos. Sci.* **31**, 1040–1052 (1974).
 - [13] P. Squires, *Tellus* **10**, 256–261 (1958).
 - [14] B. A. Albrecht, *Science* **245**, 1227 (1989).
 - [15] F. F. Abraham, *Homogeneous Nucleation Theory* (Academic, New York, 1974).
 - [16] W. J. Shugard and H. Reiss, *J. Chem. Phys.* **65**, 2827 (1976).
 - [17] S. E. Schwartz, Harshvardhan, and C. M. Benkovitz, *Proc. Natl. Acad. Sci. U.S.A.* **99**, 1784 (2002).
 - [18] P. Austin, Y. Wang, R. Pincus, and V. Kujala, *J. Atmos. Sci.* **52**, 2329 (1995).
 - [19] B. Lin and W. B. Rossow, *J. Geophys. Res.* **99**, 20 907 (1994).
 - [20] D. A. Hegg, *Geophys. Res. Lett.* **26**, 1429 (1999).
 - [21] D. Rosenfeld, *Science* **287**, 1793–1796 (2000).
 - [22] G. Falkovich, A. Fouxon, and M. G. Stepanov, *Nature (London)* **419**, 151 (2002).